Thermally activated persulfate for the chemical oxidation of chlorinated organic compounds in groundwater

Carmen M. Dominguez, Arturo Romero, David Lorenzo and Aurora Santos*

Dpto. Ingeniería Química y de Materiales, Facultad de Ciencias Químicas, Universidad Complutense Madrid. Ciudad Universitaria S/N. 28040, Madrid, Spain

Paper submitted to

Journal of Environmental Management

Special Issue **"EAAOP6"**

for consideration

* **Corresponding author' email:** aursan@ucm.es

Abstract

Chlorinated pesticides were extensively produced in the XX century, generating high amounts of toxic wastes often dumped in the surroundings of the production sites, resulting in hot points of soil and groundwater pollution worldwide. This is the case of Bailín landfill, located in Sabiñánigo (Spain), where groundwater is highly polluted with chlorobenzenes (mono, di, tri and tetra) and hexachlorocyclohexanes. This study addresses the abatement of chlorinated organic compounds (COCs) present in the groundwater coming from the Bailín landfill by thermally activated persulfate, PS (TAP). The influence of temperature (30 - 50 ºC) and oxidant concentration (2 - 40 g L^{-1}) on the efficiency of COCs (initial concentration of COCs = 57.53 mg L^{-1}, determined by the solubility of the pollutants in water) degradation has been investigated. Raising the reaction temperature and PS concentration the degradation of COCs significantly accelerates, as a result of higher production of sulfate radicals. The thermal activation of PS implies side reactions, involving the unproductive decomposition of this oxidant. The activation energy calculated for this reaction (128.48 kJ mol^{-1}) reveals that is slightly more favored by temperature than the oxidation of COCs by sulfate radicals (102.4 - 115.72 kJ mol^{-1}). At the selected operating conditions (PS = 10 g L^{-1}, 40 ºC), the almost complete conversion of COCs and a dechlorination and mineralization degree above 80% were obtained at 168 h reaction time. A kinetic model, able to adequately predict the experimental concentration of COCs when operating at different temperatures and initial concentration of PS has been proposed.

Key Words: Lindane; Chlorobenzenes; HCHs; Persulfate; Thermal activation; Oxidation.

1. Introduction

Pesticides were extensively produced and used during the last century to control a range of pests infesting the crops. Many of them have been banned owing to their long environmental persistence and acute toxicity and included in the Stockholm Convention List (Karlaganis et al., 2001; Lallas, 2001, Madaj et al., 2018). The organochlorine pesticides (OCPs) are toxic and bioaccumulative persistent organic pollutants (POPs), representing a great environmental concern nowadays (Usman et al., 2014, Khan et al., 2017, Cuozzo et al., 2018; Madaj et al., 2018). Among OCPs, lindane (γ-HexachloroCycloHexane, γ-HCH) was one of the most used pesticides in the last century. It was obtained by chlorinating benzene with an inefficient process (10 tons of wastes were generated for each ton of lindane). Lindane wastes were often dumped in the nearby of the production sites, causing hot points of soil and groundwater contamination worldwide (Vijgen et al., 2011) which has threatened human and environmental health. A recent report about lindane wastes in EU (Vega et al., 2017) explains the great concern about this problem.

Chemical oxidation is a well-established technology for the decontamination of soil and groundwater plumes with chlorinated organic compounds. It can be applied on-site to excavated soils and pumped groundwater, or *in situ* (In Situ Chemical Oxidation, ISCO). ISCO involves the injection of an oxidant in the subsurface able to react with the pollutants present in the groundwater plumes or adsorbed in the soil producing harmless substances (Siegrist et al., 2011). The selection of the oxidant should consider the nature of the contaminants and the lithological and mineralogical characteristics of the polluted site.

Among the oxidants employed in ISCO treatments (hydrogen peroxide, potassium and sodium permanganate, sodium persulfate and ozone), activated persulfate has gained interest in recent years, increasing both the research effort on this topic and its use in applications at field scale (Tsitonaki et al., 2010, Krembs et al., 2010, Yen et al., 2011, Matzek and Carter, 2016, Wacławek et al., 2017, Ike et al., 2018). The interesting properties of PS, such as i) high aqueous solubility, ii) high stability in water and/or soil, iii) relatively low cost, iv) applicable in a high pH range, v) lower affinity for natural soil organics, longer lifetime in the subsurface and higher radius of influence than hydrogen peroxide, vi) ease of handling and vii) production of benign-end products, have made it very competitive against other oxidants (Rodriguez et al., 2012; Sra et al., 2014; Devi et al., 2016, Santos et al., 2019).

The persulfate anion (E^0=2.1 V) can be activated to generate free radicals, with a significant increase in the oxidation rates of the pollutants. The activation can be accomplished i) by heat, ultraviolet (UV), microwave (MW) and ultrasound (US) (Eq. 1), ii) by adding transition metals (mainly iron cations, but also valid for other ions as Co^{2+}, Ni^{2+}, Cu^{2+}, Ru^{3+}, Ag^{+}, etc.) (Eq. 2), and iii) by using alkaline substances (alkaline activation) (Eq. 3 and Eq.4). The radical species generated depend on the pH and the activator used. As a result, sulfate radicals ($SO_4^{\cdot-}$, E^0 = 2.5-3.1 V (Ike et al., 2018, Zhu et al., 2018)) (Eq. 1), superoxide radicals ($O_2^{\cdot-}$, E^0 = -0.33 V) (Liang and Lei, 2015) (Eq. 3) and hydroxyl radicals ($OH^{\cdot}$, E^0 = 2.80 V) (Eq. 4) are generated.

$$S_2O_8^{2-} \xrightarrow{heat,UV,MW,US} 2\,SO_4^{\cdot-} \quad \text{Eq. 1}$$

$$S_2O_8^{2-} + Fe^{2+} \rightarrow Fe^{3+} + SO_4^{2-} + SO_4^{\cdot-} \quad \text{Eq. 2}$$

$$2\,S_2O_8^{2-} + 2\,H_2O \xrightarrow{OH^-} 3\,SO_4^{2-} + SO_4^{\cdot-} + O_2^{\cdot-} + 4\,H^+ \quad \text{Eq. 3}$$

$$SO_4^{\cdot -} + OH^- \rightarrow SO_4^{2-} + {}^{\cdot}OH \qquad \text{Eq. 4}$$

Thermally activated persulfate (TAP) has been suggested as a simple and clean source of sulfate radicals (Ghauch et al., 2012, Deng et al., 2013, Zhou et al., 2019) since unlike in the case of the activation with transition metals and the alkaline activation of PS, it does not require the extra addition of chemicals. Moreover, a higher amount of radical species is generated by this technique (two moles of sulfate radicals are generated per mole of persulfate, Eq.). The production rate of sulfate radicals can be modulated by controlling the reaction temperature. An increase in the temperature of the system leads to a higher rate of sulfate radical generation and therefore, of contaminants oxidation. However, it should be also considered the unproductive decomposition of PS (Goulden et al., 1978), as described in Eq. 5 (Kolthoff and Miller, 1951).

$$S_2O_8^{2-} + H_2O \rightarrow 2\,H^+ + 2\,SO_4^{2-} + \frac{1}{2}O_2 \qquad \text{Eq. 5}$$

This paper studies the effectiveness of TAP to the elimination of chlorinated organic compounds (COCs) present in the groundwater coming from the Bailín landfill, located in Sabiñanigo (Spain). The pollution was caused by the wastes of lindane production (manufactured by the company Inquinosa from 1975 to 1988), dumped in two insecure landfills. A dense non-aqueous phase liquid (DNAPL), composed mainly of chlorobenzenes and HCH isomers (Santos et al., 2018a), was generated. Due to its high density (1.5 g cm^{-3}) (Fernández et al., 2013) the DNAPL has migrated at different depths in the subsurface, being a source of continuous pollution of the groundwater (Lorenzo et al. 2020), which represent a risk for the Gallego river and the nearby receptors (Navarro et al., 2000, Fernández et al., 2013). The only work found in the bibliography studying the TAP applied to some of the cited pollutants is that by Luo (2014), who studied the abatement of chlorobenzene in spiked water.

Several technologies such as electrochemical advanced electrooxidation processes, EAOPs (Dominguez et al, 2018a, 2018b), reduction with zerovalent microparticles (Dominguez et al., 2018c) and oxidation with persulfate activated with alkali (Santos et al., 2018b) have been tested for the remediation of the groundwater of Bailín landfill. ZVIm showed low efficiency in the degradation of unsaturated compounds and the *in situ* application of this technology involves certain difficulties, aspect even more problematic in the case of EAOPs. PS activated with alkali was efficient but high reaction times were required (Santos et al., 2018b), so further research is required. Thus, in the present work, the thermal activation of PS (TAP), using mild operating conditions, has been tested for the abatement of a complex mixture of pollutants (28 COCs, including chlorobenzenes, chlorocyclohexenes, and chlorocyclohexanes) in the aqueous phase. The knowledge acquired in this study can be used for the design of an on-site treatment of the contaminated groundwater plume of the site and could also help in the development of an *in situ* treatment of the groundwater plume, although more research will be required in the last case. From our knowledge, there are no previous studies in the literature for the TAP of these compounds. The non-productive consumption of PS, a key aspect for ISCO applications and that had been scarcely studied in the bibliography up to date, has been determined. Finally, the effect of the main operating variables of the treatment, temperature and PS concentration, has been studied and a kinetic model, able to predict the experimental results, has been developed. The results here obtained will serve as the basis for the development of a future remediation process for the groundwater of Bailin landfill and other sites polluted with this kind of COCs.

2. Materials and methods

2.1 Reagents

Commercial COCs (chlorobenzene, 1,2 dichlorobenzene, 1,3 dichlorobenzene, 1,4 dichlorobenzene, 1,2,3 trichlorobenzene, 1,2,4 trichlorobenzene, 1,2,3,4 tetrachlorobenzene, 1,2,4,5 tetrachlorobenzene, 1,2,3,5 tetrachlorobenzene, pentachlorobenzene and HCH isomers) were supplied by Sigma-Aldrich. N-hexane (C_6H_{14}, Scharlau) was used for the extraction of COCs from the aqueous phase and butyl cyclohexane ($C_{10}H_{20}$) and tetrachloroethane ($C_2H_2Cl_4$) (both from Sigma-Aldrich) were used as internal standard compounds (ISTD). Potassium iodide (KI, Fisher Chemical), sodium hydrogen carbonate ($NaHCO_3$, Panreac), sodium thiosulfate pentahydrate ($Na_2S_2O_3 \cdot 5H_2O$, Sigma-Aldrich) and acetic acid ($C_2H_4O_2$, Sigma-Aldrich) were used for PS quantification. Sodium hydrogen carbonate, sodium carbonate anhydrous (Na_2CO_3, Panreac), acetone (C_3H_6O, Sigma-Aldrich), oxalic acid ($C_2H_2O_4$, Riedel-de Haën) and sulfuric acid (H_2SO_4, Fisher Chemical) were used for ion chromatography (IC) analyses. NaCl (Sigma-Aldrich) and potassium hydrogen phthalate (Nacalai Tesque) were used for IC and total organic carbon (TOC) calibration. All reagents were of analytical grade. Solutions were prepared with high-purity water obtained from a Millipore Direct-Q system with resistivity>18 MΩ cm at 25 ºC.

2.2 COCs polluted-water

The polluted water was prepared by saturating milli-Q water with DNAPL (density ≈ 1.5 g cm^{-3}) pumped from an extraction well of Bailín landfill at 35 meters below the ground level (m.g.l.) in the saturated zone (Santos et al., 2018a). For this purpose, a known volume of water was contacted with a mass of DNAPL and agitated during 24 h. Some loss of the most volatile compounds (*i.e.* chlorobenzene) can take place during this procedure. Photographs of DNAPL and the polluted water can be found in the Supplementary Material (SM Fig 1).

2.3 Oxidation runs

The oxidation runs were carried out in thermostatted cylindrical glass reactors (10 mL) with magnetic agitation (80 rpm) using a Tech-RADLEYS heating stirrer plate. The reactors were filled with 9.5 ml of polluted water and once the solution reached the reaction temperature (30, 40 and 50 ºC), 0.5 ml of the oxidant (PS) from a concentrated stock solution were added to obtain the appropriate concentration of this reagent (2, 5, 10, 20 and 40 g L^{-1}) in the reaction medium. The pH of the solution was not adjusted. To follow the evolution of the reaction, several reactors were prepared simultaneously and sacrificed for each reaction time.

Control experiments in the absence of PS were performed to evaluate the possible loss of COCs by volatilization at the different temperatures tested. The unproductive consumption of PS by thermal effect was also evaluated at the three temperatures studied. A table summarizing the experiments carried out, including the operating conditions selected (COCs concentration, temperature, PS concentration, the relation between the experimental concentration of PS and the stoichiometric value for the mineralization of COCs and initial pH) is collected in SM Table 1. The addition of PS to the reaction medium (from a concentrated stock solution previously prepared), provokes a decrease in the initial pH of the solution from circumneutral values (pH ≈ 6.5-7) to acid values due to the release of protons to the liquid phase (Eq. 5), the resulting pH depending on the initial concentration of PS. Thus, the initial pH of the experiments carried out with an initial concentration of PS of 40 g L^{-1} was 3 ± 0.1. When lower concentrations of PS were used, the initial pH of the solution was in the range 3.6 – 3. The stoichiometric oxidation reactions between PS and the different families of COCs are collected in SM Table 2. It should be noted that the oxidation experiments have been performed in a wide range of

PS concentration, as usually found in the bibliography for this kind of treatments (Huang et al., 2005, Ma et al., 2018, Wang et al., 2018, Matzek and Carter, 2016). The aim of using oxidant concentrations higher than the stoichiometric amount required for the mineralization of COCs is to decrease the reaction times required and to ensure a high enough radius of influence of PS transportation in groundwater if an in situ-treatment is carried out.

All the experiments were performed by duplicate and the standard deviation was always less than 10%.

2.4 Analytical methods

The identification and quantification of COCs (HCH isomers, as well as chlorobenzenes, and other cyclic non-aromatic chlorinated compounds) in the starting polluted water was carried out by gas chromatography coupled with a flame ionization detector (GC-FID) and confirmed with an electron capture detector (GC-ECD) using a HP-5-MS column. Helium was used as the carrier gas, with a flow rate of 2.8 mL min^{-1}. The GC injection port temperature was set at 180 °C (the injection volume was 2 µL). The temperature program started at 80 °C followed by a temperature ramp of 10 °C min^{-1} to 310 °C and then, held constant for 1 min. Before chromatographic analyses, water samples were extracted with the same mass of n-hexane (liquid-liquid extraction). After vigorous agitation, the supernatant organic phase was taken and analyzed. To minimize experimental errors in COCs quantification, butyl cyclohexane and tetrachloroethane were added to the extracted samples as internal standard compounds (ISTD 1 and ISTD 2, respectively). COCs calibration in the range 0.025-20 mg L^{-1} was previously performed by dissolving standards of commercial COCs directly in n-hexane. GC-FID response

factors used for COCs without commercial standards available were obtained of commercial compounds with similar chemical structure and number of chlorines.

The concentration of PS in solution was determined by iodometric titration with sodium thiosulfate, by using a potentiometric titration analyzer supplied by Metrohm (Ti Amo 2.3). The detection limit of PS by this technique was 10 mg L^{-1}. The dechlorination degree of the polluted water was evaluated in terms of chlorides released to the liquid phase (detection limit of chlorides = 0.1 mg L^{-1}), which were quantified by ion chromatography (Metrohm 761 Compact IC) with chemical suppression coupled to a conductivity detector. A Metrosep A SUPP5 5-250 column (25 cm length, 4 mm diameter) was used as stationary phase and an aqueous solution 3.2 mmol L^{-1} of Na_2CO_3 and 1 mmol L^{-1} of $NaHCO_3$ (0.7 mL min^{-1}) as mobile phase. The injection system included an online filtering system (0.45 μm). The measure of carboxylic acids at the end of the reactions, possible byproducts of COCs oxidation, were also determined by this technique.

The decay in TOC solution was measured by a Shimadzu TOC-V_{CSH} analyzer. Reproducible TOC values with an accuracy of ± 2% were determined. TOC calibration was previously performed with potassium hydrogen phthalate solutions in the range 0.1 - 100 mg L^{-1}. The pH of the samples at the beginning and the end of the TAP treatment was measured using a Basic 20-CRISON pH electrode.

3. Results

3.1 COCs polluted water characterization

The polluted water obtained by saturation with the organic phase (DNAPL) from the Bailin landfill was a colorless liquid sample with a neutral pH value (pH ≈ 6.5). SM Table 3 summarizes the main information about the identified pollutants the chemical formula, the acronym used for each COC and its concentration (in mg L^{-1}). 28 different COCs have

been identified and quantified; the sum of them being 57.53 mg·L^{-1}, which represents a TOC concentration of 26.41 mg L^{-1}.

The composition of the simulated water was similar to the groundwater of the landfill (Santos et al. 2018a, Lorenzo et al., 2020) but with a lower concentration of CB due to the partial volatilization of this compound during the preparation of the simulated polluted groundwater. The GC-FID and GC-ECD chromatogram of the polluted sample before the oxidation treatment with the chemical structure of the identified COCs is shown in SM Fig 2.

The positional isomers of the same COC, listed SM Table 3, have been gathered as a generic compound. Thus, the families of COCs and their global concentration are summarized in Table 1.

Table 1. COCs families, defined as the sum of the positional isomers, and their initial concentration in the starting polluted water.

COC family	$\mathbf{C_j}$ ($\mathbf{mg\ L^{-1}}$)
CB	25.76
DCB	5.54
TCB	2.57
TetraCB	0.60
PCB	0.02
PentaCX	6.18
HexaCX	0.56
HeptaCH	2.50
HCH	13.80

3.2 Preliminary tests: thermal decomposition of PS and COCs volatilization

As previously seen in the introduction section, PS decomposes generating sulfate radicals by temperature effect (Eq. 1). Although knowing the stability of the oxidant is determinant for *in situ* applications, the thermal unproductive decomposition of PS has been scarcely studied in the bibliography (Wang et al., 2017, Santos et al., 2019). Here, the stability of PS in the aqueous phase (in the absence of COCs) has been evaluated at 30, 40 and 50 ºC (R1, R2 and R3, respectively). The PS conversion with experimental time at each temperature has been depicted in Fig. 1. As expected, an increase in the temperature of the system implied an increase in the rate of oxidant unproductive decomposition. Accordingly, the pH measured at the end of these experiments decreased with increasing the temperature, as a result of proton release (Eq. 5). Thus, in the experiment carried out at 50 ºC, that one with the highest conversion of PS (≈ 80% at 144 h reaction time), the final pH was 1.36.

Otherwise, in runs carried out in the absence of PS at 30, 40 and 50 ºC (R4, R5 and R6, respectively) a negligible change of COCs concentration due to volatilization was found during the experimental time (144 h). At the highest temperature tested this loss was less than 15% for any of the COCs family (data not shown). This fact proved that losses of COCs by volatilization can be minimized using reactors (glass vials) without head-space.

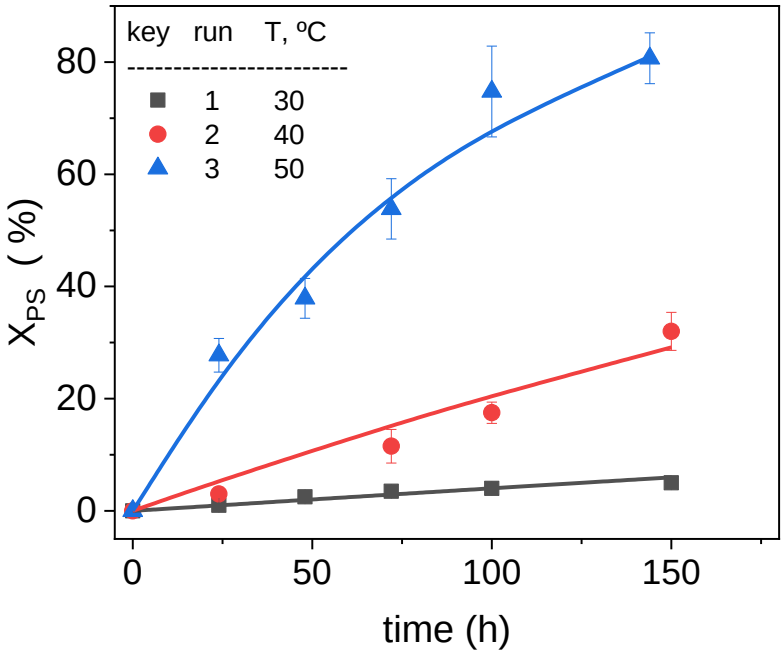

Figure 1. PS (40 g L^{-1}) decomposition by thermal effect in the absence of pollutants at different temperatures (R1, R2 and R3, SM Table 1). Experimental data as symbols and predicted values, using Eq. 20 and the kinetic parameters shown in Table 2, are plotted as lines.

3.3 Temperature effect on COCs degradation

The conversion of each COCs family with reaction time by oxidation with PS (40 g L^{-1}) thermally activated at T=30 (a), T=40 (b), and T=50ºC (c) is shown in Fig. 2 (R7, R8 and R9). The conversion profile obtained for TetraCBs, PentaCXs, HCHs, HexaCXs and HeptaCHs was very similar during the experimental time, so these families of COCs have been lumped and the conversion of them named X_{lump} (Eq. 6).

$$X_{lump} = 1 - \frac{c_j}{c_{j,o}} \quad j = TetraCBs, PentaCXs, HCHs, HexaCX, HeptaCHs \qquad \text{Eq. 6}$$

being c_j the concentration (mmol L^{-1}) of a COCs family (sum of all isomers) at time *t*, and $c_{j,0}$, the initial concentration (mmol L^{-1}) of a COCs family.

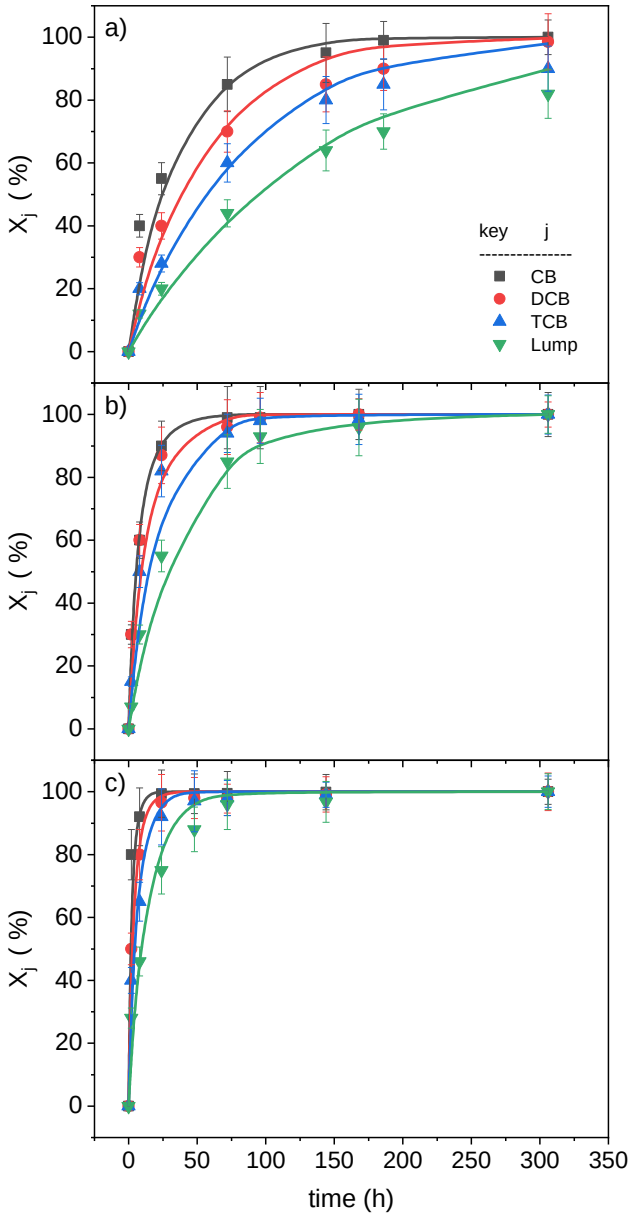

Figure 2. Conversion of COCs (grouped by families) during their oxidation by PS activated at a) 30ºC, b) 40ºC, c) 50ºC (R7, R8, R9, SM Table 1, $COCs_0$=57.53 mg L^{-1}, PS_0=40 g L^{-1}). Experimental data as symbols and predicted values using Eq. 23 and the kinetic parameters shown in Table 2 and Table 3, are plotted as lines.

Firstly, it should be noted that the thermal activation of PS under the operating conditions tested (pH below 3, see SM Table 1) generates predominantly sulfate radicals, which are responsible for COCs oxidation (Liang and Su, 2009, Furman et al., 2011, Ma et al., 2017). Thus, it has been reported that sulfate radical is predominantly present at pH $\leq$ 3; both sulfate and hydroxyl radicals are present in the pH range between 3 and 9; and hydroxyl radical is predominantly present at a pH of 12 (Liang and Su, 2009). Therefore, the role of hydroxyl radicals can be neglected in this study.

As can be seen, the different COCs families were progressively abated by the thermal activation of PS with reaction time. The GC-FID and GC-ECD chromatograms of the polluted water treated at 40 ºC at 24 (in red) and 72 h (in blue) reaction time can be seen in SM Fig. 2. The chromatographic peaks corresponding to the COCs were significantly reduced, achieving a global conversion of COCs above 95% at 72 h reaction time. These results demonstrated the high efficiency of TAP oxidation in the degradation of such recalcitrant compounds.

Given the results obtained, it can be firstly concluded that as the chlorine content of the COC increases, the pollutant resulted to be more resistant to PS oxidation, obtaining the following conversion ranking: $X_{CB} > X_{DCBs} > X_{TCBs} > X_{lump}$ regardless of the temperature tested. Thus, at 72 h reaction time, the conversion of these families of COCs at 30 ºC were 85, 70, 60 and 44%, respectively. This behavior was previously observed in the oxidation of chlorinated organic compounds from lindane wastes by the combination of non-ionic surfactant soil flushing and Fenton oxidation (Dominguez et al., 2018d).

Secondly, it has been demonstrated that temperature plays an important role in the degradation of COCs. Increasing the reaction temperature, the production rate of sulfate radicals increases and therefore, the oxidation of the pollutants. The influence of

temperature is noted regardless of the family of COCs. Raising the reaction temperature from 30 to 40 ºC, the degradation of COCs is significantly favored. The global conversion of COCs at 72 h increased from 73.1% to 99.7% when raising the temperature from 30 to 40 ºC (Fig. 3). However, working at higher temperatures (50 ºC) leads to equivalent results (similar conversion profiles of COCs families were obtained, Fig. 2b and Fig. 2c), and therefore, in this scenario, the employ of temperatures above 40 ºC seems to be not recommendable.

Intermediate chlorinated organic compounds (different from the starting ones) at significant amounts were not detected by GC-FID and GC-ECD analyses (the last one, very sensible towards chlorinated compounds) during the TAP treatment (see SM Fig. 2), where additional chromatographic peaks different to those initially identified did not appear. Only formic acid was detected as oxidation by-product by ion chromatography. Therefore, from these results and according to bibliographic data, a substantial reduction in toxicity of the treated water can be estimated after the oxidation treatment. The starting organic pollutants: chlorobenzenes and non-aromatic cyclic chlorinated compounds (pentachlorocyclohexenes, hexachlorocyclohexanes, heptachlorocyclohexenes and hexachlorocyclohexenes) are highly toxic and persistent organic compounds (Calamari et al., 1983, Nolan et al., 2012, Fernández et al., 2013, Santos et al., 2018a). As a result of their oxidation by the action of sulfate radicals, these compounds are dechlorinated and broken down to other short chain oxidized compounds, such as formic acid, and eventually mineralized (CO2, H2O and Cl-), with the consequent reduction of toxicity (see SM Table 4, where the effective nominal concentration of toxicant values, EC50, found in the bibliography by *Vibrio Fischeri* analyses for the compounds of interest, obtained at 15 min of exposure time, are collected). Moreover, not only the reduction of

this acute toxicity should be considered; the loss of chlorine in the organic molecules greatly diminish their harmful and carcinogenic potential, which is even more important.

Theoretically, bonded chloride ions should be converted to free chloride ions as a result of COCs degradation. Thus, the complete oxidation of COCs by sulfate radicals gives carbon dioxide, water and chlorides as final compounds (SM Table 2). Thereby, the extent of chloride ion is provided as an indication of the cleavage of carbon-chloride bond in the degradation of chlorinated contaminants and, together with the mineralization degree, they are used to evaluate the efficiency of the oxidation treatments. Both parameters (mineralization and dechlorination) have been determined at the three temperatures tested and the results obtained at 72 h are shown in Fig. 3. The dechlorination degree has been expressed as the relative amount of chlorides measured in the liquid medium normalized by the total chlorine content of the initial sample (calculated as the sum of the chlorine content of the individual COCs). The global conversion of COCs at this reaction time has been also included. The differences obtained between the conversion of COCs and the dechlorination degree are mainly attributed to analysis errors due to interference with the measurement of other ions, such as sulfates, by ion chromatography.

As well as occurred with the conversion of pollutants, the degree of mineralization and dechlorination increased significantly as the temperature increased from 30 to 40 °C. However, increasing the temperature up to 50 °C does not mean a significant improvement in the results obtained but implies an unaffordable increase in cost. Moreover, to select the optimal temperature range in TAP, not only the degradation of the contaminant must be taken into account. It should be considered that the rate of PS unproductive decomposition can increases more rapidly than the rate of organic substrates

oxidation (see section 3.5). Therefore, taking these aspects into account, as well as the costs of the process, 40 ºC has been selected as the most appropriate temperature.

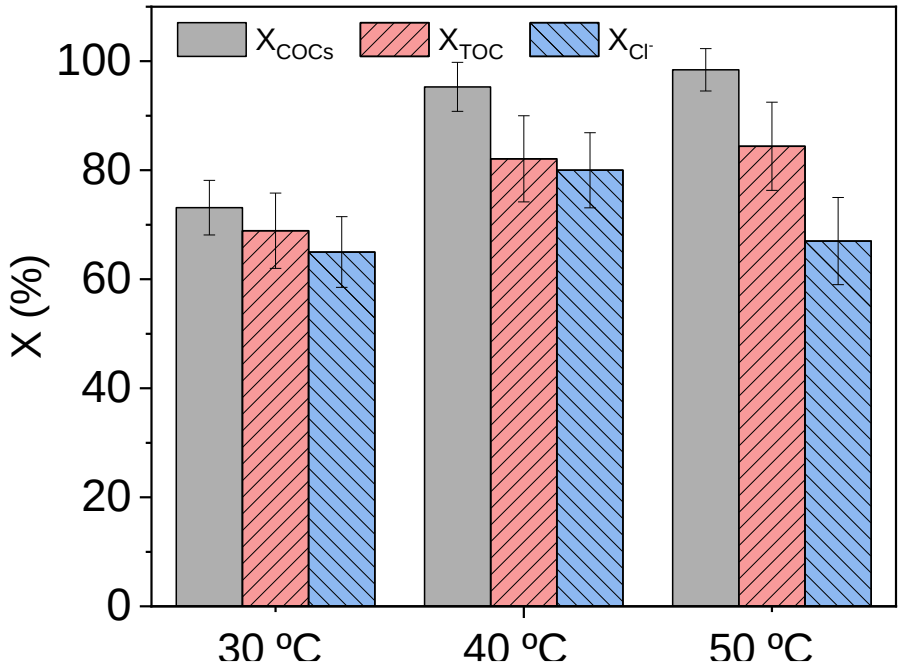

Figure 3. COCs oxidation, mineralization and dechlorination by thermal activated PS at 72 h reaction time at different temperatures (R7, R8, R9, SM Table 1, $COCs_0$=57.53 mg L^{-1}, PS_0=40 g L^{-1}).

The effect of pollutants on PS decomposition has also been analyzed. For that purpose, the conversion of PS in the presence (R7, R8 and R9) and the absence (R1, R2 and R3) of COCs has been compared (the results obtained at 72 and 144 h reaction time have been included in SM Fig. 3). At the same temperature studied there are only slight differences in the consumption of PS in the presence or absence of organics. Moreover, the decrease in pH solution was equivalent in these runs. This fact might be related with the high excess of the oxidant used ($C_{PS} \approx 34\ C_{PS}^{stq}$), being C_{PS}^{stq} the concentration theoretically required for COCs mineralization. These results (similar rate of PS self-degradation and PS

decomposition in the presence of organic compounds) indicate that sulfate radicals are responsible for the degradation of COCs (Liang and Su, 2009).

3.4 PS concentration effect on COCs degradation

Once the efficiency of TAP on the degradation of COCs has been demonstrated using a high concentration of the oxidant (40 g L^{-1}), a systematic study varying the concentration of PS was performed to optimize the consumption of this reagent and, therefore, reduce the operating costs. Five concentrations of PS (2, 5, 10, 20 and 40 g L^{-1}, R10, R11, R12, R13 and R8, respectively), always above the stoichiometric amount (C_{PS}/C_{PS}^{stq} between 2.1 and 34) were tested. The results obtained have been grouped by COCs families and depicted in Fig. 4, where the corresponding concentration of PS (g L^{-1}) is given. Moreover, the conversion of the sum of COCs at different oxidant concentrations has been also depicted in Fig. 5a. The evolution of PS conversion with reaction time in these experiments is shown in Fig. 5b.

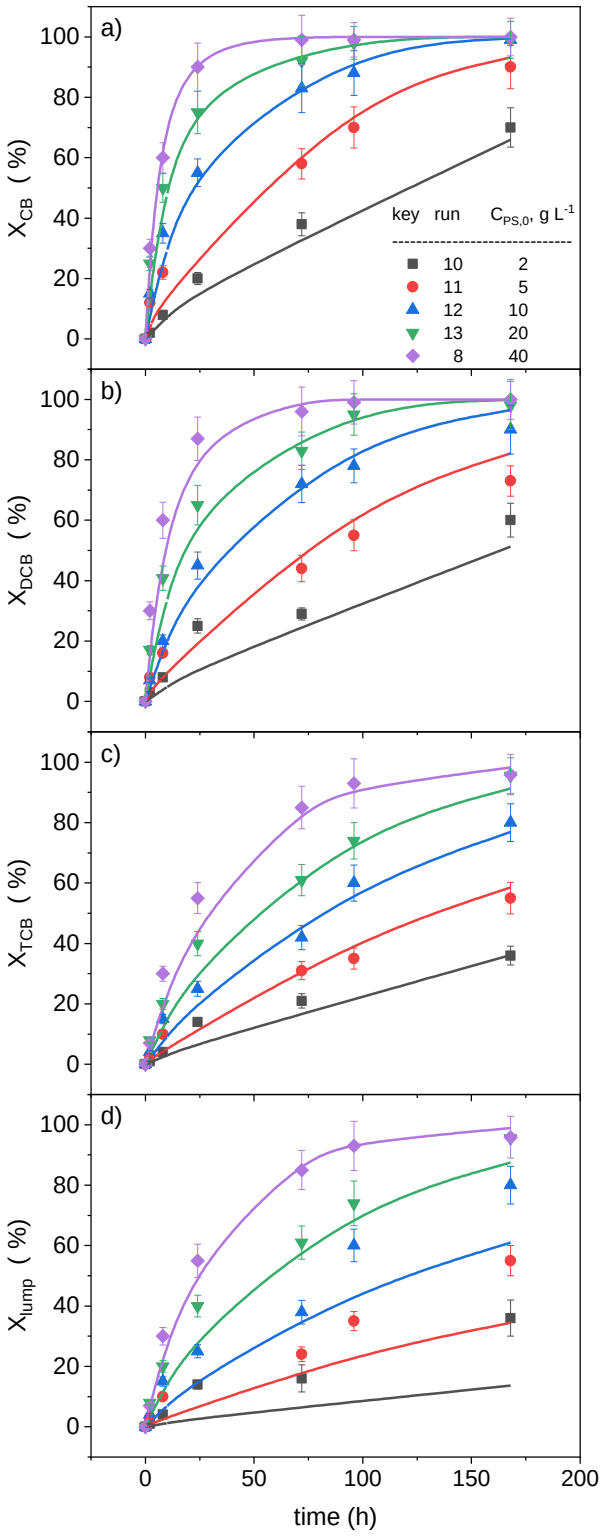

Figure 4. Conversion of families of COCs with time at T = 40ºC and different initial concentrations of PS (g L^{-1}): (a) CB, (b) DCB), (c) TCB, (d) lumped species defined in

Eq. 6 (R8, SM Table 1). Experimental data as symbols and predicted values using Eq. 23 and the kinetic parameters shown in Table 2 and Table 3 are plotted as lines.

As can be seen in Fig. 4 and Fig. 5a, as the initial concentration of PS increases, the degradation rate of the contaminants increases, due to a higher production of sulfate radicals. These results are in accordance with those reported in the bibliography relative to other organic pollutants by TAP (Huang et al., 2002, Liang et al., 2003, Deng et al., 2013, Luo 2014, Ji et al., 2015) and also with other PS activation methods (Romero et al., 2010; Zhao et al., 2014; Ji et al., 2015; Santos et al., 2018b). At 168 h reaction time, COCs were almost dechlorinated when working with an initial concentration of PS $\geq$ 10 g L^{-1}. The conversion of PS was independent of its initial concentration (Fig. 5b), confirming that oxidant decomposition follows first-order reaction (Huang et al., 2002, Liang, et al., 2003, Waldemer et al., 2007, Liang and Su, 2009) (see section 3.5). Therefore, the final pH value decreased with the initial concentration of PS, obtaining pH values at the end of the treatment between 1.36 and 1.95.

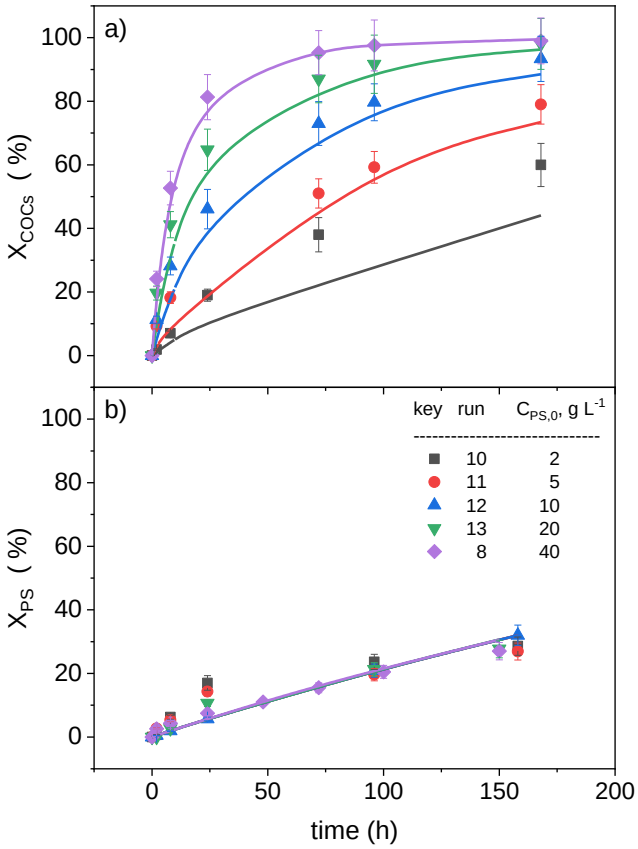

Figure 5. Conversion of a) Sum of COCs and b) PS with time at 40 ºC with different initial concentrations of PS (g L^{-1}) (R8, R10, R11, R12 and R13, SM Table 1), $COCs_0$=57.53 mg L^{-1}). Experimental data as symbols and predicted values using Eq. 20 and Eq. 23 and the kinetic parameters shown in Table 2 and Table 3, are plotted as lines.

Finally, the conversion of the sum COCs, as well as the mineralization and dechlorination degree, obtained at 72 h reaction time when working with different initial concentrations of PS are depicted in Fig. 6.

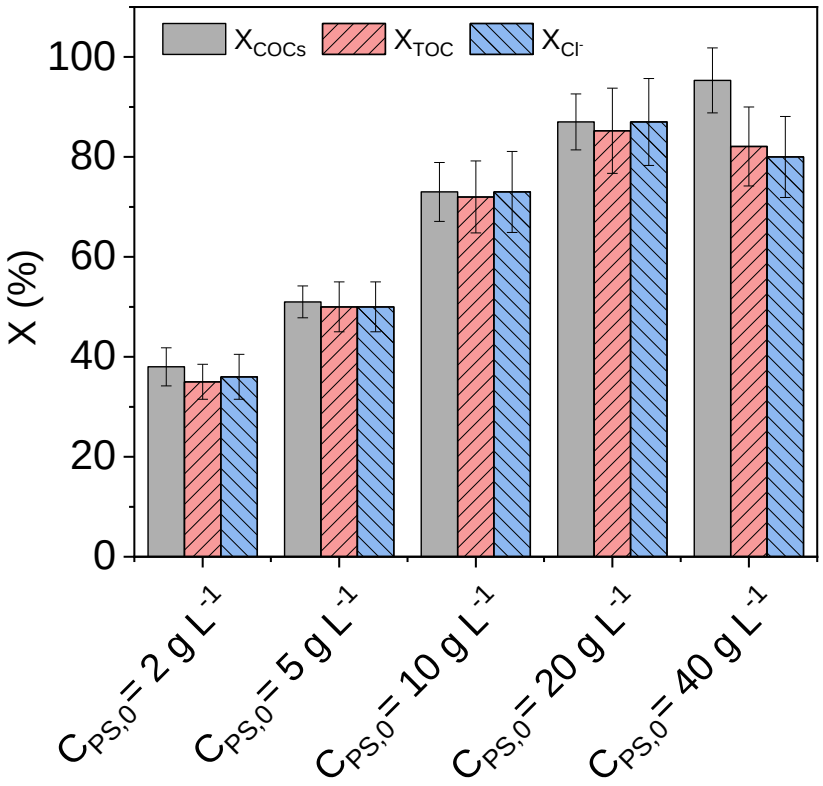

Figure 6. COCs oxidation, mineralization and dechlorination by TAP at 40 ºC and 72 h reaction time with different initial concentration of PS (R8, R10, R11, R12 and R13, SM Table 1), $COCs_0$=57.53 mg L^{-1}).

The higher the oxidant concentration the higher the conversion of the sum of COCs, the TOC abatement and the dechlorination degree. Considering that PS is quite stable at 40ºC, the optimal PS concentration must be chosen considering the cost of the reagent and the time saved to reach the desired degree of pollutants conversion.

The results obtained here in an aqueous system are promising for the on-site treatment of the pumped groundwater. Moreover, due to the low unproductive consumption of PS by the soil (Lominchar et al. 2018), these results encourage additional studies of the on-site remediation of excavated soils polluted with chlorobenzenes and HCHs by TAP.

Additionally, the *in situ* application of this process at field scale, would be technically feasible using different technologies such as radio frequency or electrical resistance to warm up select portions of the polluted aquifer, in which the oxidant had been previously dosed. The application of this technology for the treatment of contaminants *in situ* or on-site will be a function of the determined characteristics of each case of contamination and further studies at pilot scale will be required to evaluate the cost and viability of the process.

Regarding the treatment cost, both energy and oxidant costs should be taken into account. Brown et al. (2003) provide some information to compare the costs of several oxidant systems for groundwater remediation. TAP can be considered as an effective treatment with moderate cost, at least in the case of on-site applications. However, to evaluate the efficiency and economy of TAP treatment, the application of other AOPs to the treatment of the complex mixture of chlorinated organic compounds here studied should be carried out. In this sense, the work of Bolton et al. (1996) could be of great help.

If an on-site treatment of the pumped groundwater is carried out with TAP, the resulting concentration of sulfate in the treated water should also be considered to design the final disposal of this aqueous phase. It can be reinjected in the subsurface or it can be used to treat polluted excavated soils on-site. If the aqueous phase obtained after the TAP treatment is discarded in superficial water o is sent to a wastewater treatment plant, a specific treatment to decrease the sulfate concentration could be implemented if necessary.

3.5. Kinetic model.

The abatement of COCs in the aqueous phase using thermally activated persulfate is based on the production of sulfate radicals (Liang and Bruell, 2008), as shown Eq. 7 (Eq. 1

particularized for TAP). Sulfate radical is a strong oxidant accepting an electron to produce the sulfate anion $(SO_4)^{2-}$ (Eq. 8), the reduction of the sulfate radical resulting from the oxidation of COCs.

$$(S_2O_4)^{2-} \xrightarrow{heat} 2SO_4^{\cdot-} \quad \text{Eq. 7}$$

$$SO_4^{\cdot-} + 1e^- \rightarrow (SO_4)^{2-} \quad \text{Eq. 8}$$

The reaction network considered to model the COCs oxidation by TAP involved the families of CB, DCB, TCB and the COCs gathered as lumped compounds in Eq. 6. The reaction of each COC with PS takes place in a parallel reaction scheme (Eq. 9 to Eq. 12):

$$r_1: C_6H_5Cl\ (CB) + \upsilon_{1,PS}\ SO_4^{\cdot-} \rightarrow products \quad \text{Eq. 9}$$

$$r_2: C_6H_4Cl_2\ (DCB) + \upsilon_{2,PS}\ SO_4^{\cdot-} \rightarrow products \quad \text{Eq. 10}$$

$$r_3: C_6H_3Cl_3\ (TCB) + \upsilon_{3,PS}\ SO_4^{\cdot-} \rightarrow products \quad \text{Eq. 11}$$

$$r_4: C_nH_mCl_l\ (lump\ in\ Eq.6) + \upsilon_{4,PS}\ SO_4^{\cdot-} \rightarrow products \quad \text{Eq. 12}$$

The activation of persulfate takes place following two reactions in parallel: a reaction that results in the production of sulfate radicals (Eq. 1) and the unproductive reaction expressed in Eq. 5. These reactions cannot be isolated, so they have been lumped in Eq. 13:

$$r_5: (S_2O_8)^{2-} + H_2O \xrightarrow{Heat} products \quad \text{Eq. 13}$$

As explained before, the concentration of PS used in runs 7 - 13 was much higher than the stoichiometric concentration needed to achieve the complete mineralization of COCs. Therefore, PS is the excess reagent.

The kinetic model considered a set of 4 reactions whose overall reaction rates were summarized in Eq. 14.

$$r_i = k_i \cdot (C_{PS})^{n_i} \cdot \left(C_j\right)^{m_i} \quad \text{Eq. 14}$$

where r_i, is the overall reaction rate of i reaction, in $mmol\ L^{-1}\ h^{-1}$, C_{PS} is the PS concentration, in $mmol\ L^{-1}$, at a reaction time = *t*, and C_j is the molar concentration of COC j involved in the reaction i (represented in Eq. 9 to Eq. 12), k_i is the kinetic constant and n_i and m_i, the reaction partial order for PS and COC concentration, respectively.

The overall reaction rate of the non-desired reaction of PS, which means a non-productive reaction, is represented as follows:

$$r_5 = k_5 \cdot C_{PS} \quad \text{Eq. 15}$$

To consider the temperature effect experimentally observed, the kinetic constant of each reaction rate (r_1 to r_5), k_i, can be expressed by the Arrhenius equation:

$$k_i = k_{0,i} \cdot \exp\left(-\frac{Ea_i}{RT}\right) \quad \text{Eq. 16}$$

where $k_{0,i}$ is the preexponential factor, Ea_i is the activation energy ($kJ\ mol^{-1}$), R is the universal gas constant ($kJ\ mol^{-1}\ K^{-1}$), and T is the absolute reaction temperature (K).

The mass balance for the concentration of COCs ($mmol\ L^{-1}$) in the batch reactor, assuming perfect mixing, can be described as follows:

$$\frac{dC_j}{dt} = R_j = -r_i = -k_i \cdot (C_{PS})^{n_i} \cdot \left(C_j\right)^{m_i} \quad \text{Eq. 17}$$

being R_j and C_j, the production rate of the compound j ($mmol\,L^{-1}\,h^{-1}$) and the concentration of j, respectively.

The mass balance of PS must consider the activation and unproductive reactions (lumped in Eq. 13) and the PS consumed in COCs oxidation reactions ($r_1$to r_9, SM Table 2):

$$\frac{dC_{PS}}{dt} = R_{PS} = -r_5 - \sum_{i=1}^{4} v_{i,PS} \cdot r_i \qquad \text{Eq. 18}$$

being $v_{i,PS}$ the stoichiometric coefficient of PS in reactions $r_1$to r_4 (Eq. 9 to Eq. 12). However, since a high excess of PS regarding to that one required for COCs mineralization was used, the last term of Eq. 18 can be neglected in the mass balance of PS.

3.5.1. Kinetics of non-productive PS reaction.

The activation of PS involves two parallel reactions (the sulfate radicals production and the unproductive decomposition of PS). Both reactions are lumped in Eq. 13, and it can be described by first-order reaction kinetics (Eq. 15) in the absence of pollutants, as previously reported in the literature (Liang, et al., 2003, Wang et al. 2017, Santos et al., 2019). In runs 1-3, only PS was used within the temperature range 30-50 ºC, and thus, Eq. 18 can be simplified in Eq. 19 (COCs were not involved in the reaction).

$$\frac{dC_{PS}}{dt} = R_{PS} = -r_5 = -k_5 \cdot C_{PS} \qquad \text{Eq. 19}$$

being k_5 the sum of kinetic constants of reactions in Eq. 7 and Eq. ,5 considering that they are first-order reaction kinetics.

Then, the concentration of PS with reaction time in the absence of COCs can be predicted by integrating Eq. 19 and, therefore, also the conversion of PS:

$$1 - X_{PS} = exp\left(-k_{o5}\, exp\left(-\frac{E_{a5}}{RT}\right) t\right) \quad \text{Eq. 20}$$

Experimental values obtained for PS conversion *vs.* reaction time, in runs 1 to 3, were fitted to Eq. 20. Values of Ea_5 and $k_{0,5}$ were estimated by using a gPROMS tool, based on the Maximum Likelihood formulation, which provides a simultaneous estimation of parameters to determine values for the uncertain physical and variance model parameters, maximizing the probability that the mathematical model will predict the measured values obtained from the experiments to minimize the sum of quadratic errors between both values, expressed in Eq. 21.

$$SQR = \sum \left(X_{exp} - X_{pred}\right)^2 \quad \text{Eq. 21}$$

The kinetic parameters $k_{o,5}$ and E_{a5}, obtained by data fitting, are summarized in Table 2. Residual sum of squares (SQR) was calculated by comparison of experimental data to those predicted by the kinetic model. The confidence intervals (CI) of the estimated kinetic parameters at 95% are also provided in Table 2.

Table 2. Kinetic parameters of thermal unproductive decomposition of PS estimated by fitting data in runs 1-3 to Eq. 20.

Parameter	**Value ±CI 95%***
$Ea_5, kJ\ mol^{-1}$	128.48 ± 0.03
$k_{0,5}, h^{-1}$	$6.25 \cdot 10^{18} \pm 6.4 \cdot 10^{16}$
SQR	119

* 95 % Confidence Interval

The estimated activation energy of PS thermal decomposition was 128.48 kJ mol^{-1}. This value is very close to that reported by Devi et al (2016) for the thermal activation of PS (E_a = 140.16 kJ mol^{-1}) in an interesting work in which hydrogen peroxide and persulfate treatments in wastewater systems were revised (Devi et al., 2016).

Therefore, the kinetic equation for the thermal unproductive decomposition of PS can be given by the following expression:

$$r_5\left(\frac{mmol}{L\,h}\right) = 6.25 \cdot 10^{18} \cdot \exp\left(\frac{-128.48}{R \cdot T}\right) \cdot C_{PS}(mmol\,L^{-1}) \qquad \text{Eq. 22}$$

Values of PS concentration predicted by using Eq. 20, are represented as lines in Fig. 1. As can be seen, a good agreement between experimental and predicted values was found, confirming the validity of the kinetic model proposed.

3.5.2. Kinetic model of COCs abatement

Data from runs 7 to 9, carried out at the same oxidant concentration but using different temperatures, and data from run 8 and runs 10-13, carried out at T=40ºC and different initial concentrations of PS, have been simultaneously analyzed to obtain the kinetic parameters in r_1 to r_5. As an initial approach, it was considered that the reaction order for each family of COCs was close to the unity ($m_i = 1$). On the other hand, a stoichiometric excess of PS was used in all the experiments and similar PS conversions were obtained with and without COCs at the experimental conditions studied. Therefore, the mass balance of PS in Eq. 18 can be simplified to that expressed in Eq. 20 with the kinetic parameters shown in Table 2.

Considering the previous hypothesis, the mass balance of COCs (Eq. 17) can be written as follows:

$$\frac{dX_j}{dt} = k_{io} \exp\left(-\frac{E_{ai}}{RT}\right) \cdot \left[C_{Pso} \exp\left(-k_{o,5} \exp\left(-\frac{E_{a5}}{RT}\right) t\right)\right]^{ni} \cdot (1 - X_j) \qquad \text{Eq. 23}$$

Conversion data of each family of COCs in runs 7 to 13 have been fitted simultaneously to Eq. 23 using the gPROMS tool. Values of $k_{o,5}$ and E_{a5} were those shown in Table 2

and estimated values of k_{io}, E_{ai} and n_i are summarized in Table 3. In this table, the confidence of interval of each parameters and the sum of Residual Sum of Squares, calculated by Eq. 21 for all COCs families, are also shown.

Table 3. Kinetic parameters for COCs abatement using thermally activated PS. Values estimated by fitting experimental data $X_j\ vs.\ t$ in runs 7 to 13 to Eq. 22

i	j	$Ea_i \pm CI$ $kJ\ mol^{-1}$	$k_{0,i} \pm CI$ $L \cdot mmol^{-1}\ h^{-1}$	$n_i \pm CI$
1	CB	115.72 ± 0.03	$1.42 \cdot 10^{17} \pm 4.35 \cdot 10^{15}$	1.001 ± 0.0001
2	DCB	114.82 ± 0.03	$9.72 \cdot 10^{15} \pm 2.12 \cdot 10^{12}$	1.012 ± 0.0001
3	TCB	110.30 ± 0.02	$9.47 \cdot 10^{14} \pm 1.98 \cdot 10^{11}$	0.950 ± 0.0001
4	lump	102.40 ± 0.02	$2.49 \cdot 10^{13} \pm 4.83 \cdot 10^{10}$	1.001 ± 0.0001
SQR= 6914				

As can be seen, the activation energies of the COCs oxidation by TAP are slightly lower than the corresponding to the unproductive decomposition of PS by thermal effects. This means that an increase of temperature selectively favored the unproductive consumption of PS over the COCs oxidation rate. As can be seen in Table 3, the value of n_i is close to the unity for all the COCs families studied. The value of activation energy in the TAP of spiked water with CB found in literature was 97.34 kJ mol^{-1} (Luo 2014), that is in the range of that reported here.

The predicted values using Eq. 23 and kinetic parameters shown in Tables 2 and 3 are plotted in Fig. 2, Fig. 4 and Fig. 5 as lines. As can be seen, a good agreement between the experimental and predicted values was found.

4. Conclusions

The results obtained in the present work show that thermally activated PS (TAP) treatment is effective for the abatement of chlorobenzenes (mono, di, tri, tetra) and HCHs in the aqueous phase. It has been obtained that the higher the chlorine content of the COC,

the higher resistance towards oxidation, obtaining the following conversion ranking: $X_{CB} > X_{DCBs} > X_{TCBs} > X_{lump}$ regardless of the temperature tested. The temperature notably increases the kinetics of the oxidation of the pollutants, but also the thermal decomposition of PS. From the activation energies calculated, it was found that the rate of the unproductive consumption of PS was selectively increased with the temperature rise. Moreover, it was found that the higher PS concentration (always above the stoichiometric amount for the mineralization of the pollutants) the higher the COCs abatement. However, as PS can remain in the reaction media during long times at moderate temperatures, the selection of the optimal PS concentration and temperature will require a detailed analysis that considers the cost of the oxidant and the time required to achieve the remediation goal. As an example, using a PS concentration around 10 g L^{-1} and a temperature of 40 ºC, 95% of COCs conversion was achieved and with a decomposition of PS lower than 40% (168 h). The dechlorination and mineralization degree was around 80% at this reaction time Moreover, it was verified that no chlorinated organic compounds as oxidation byproducts were generated during the treatment. Therefore, although further research is required, TAP of chlorobenzenes and HCHs could be proposed as an on-site or *in situ* treatment to remediate the polluted site.

Finally, a kinetic model for the thermal decomposition rate of PS and the oxidation rate of each family of COCs has been proposed and validated, considering the effects of PS and COC concentration and temperature in the reaction rates. The kinetic model explains adequately the experimental results and can be very helpful to design a TAP treatment for the destruction of chlorobenzenes and HCHs at the experimental variable ranges here studied.

Acknowledgments

The authors acknowledge financial support from Regional Government of Madrid, project CARESOIL (S2018/EMT-4317) and from the Spanish Ministry of Science, project CTM2016-77151-C2-1-R. The authors thank the Department of Climate Change and Environmental Education, Government of Aragon, for their support during this work. Carmen M. Dominguez acknowledges the Spanish MINECO for the "Juan de la Cierva" post-doctoral contract (FJCI-2016-28462).

Notation

Symbols

C_j = molar concentration of compound *j*, $mmol\ kg^{-1}$

Ea_i= activation energy of reaction i, $kJ \cdot mol^{-1}$

k_5= kinetic constant of reaction 5 of unproductive PS decomposition, h^{-1}

$k_{5,0}$= kinetic preexponential constant of reaction 5 of unproductive PS decomposition, h^{-1}

k_i= kinetic constant of reaction i, $mmol\ L^{-1}h^{-1}$

$k_{i,0}$= kinetic preexponential constant of reaction i, $mmol\ L^{-1}h^{-1}$

M_j = molecular weight, $mol\ g^{-1}$

r_i = reaction rate for the *k* reaction, $mmol\ L^{-1}\ h^{-1}$

R_j = molar flux rate of j compound, $mmol\ L^{-1}\ h^{-1}$

T = temperature, K

X_j = conversion of compound *j*

n_j = mol of compound *j*

Subscripts

j = compounds

i = reaction number.

0 = initial

f = final

Superscripts

stq =stochiometric

References

Bolton, J. R., Bircher, K. G., Tumas, W., Tolman, C. A. (1996). Figures-of-merit for the technical development and application of advanced oxidation processes. Journal of advanced oxidation technologies, 1(1), 13-17.

Brown, R. A. (2003). In situ chemical oxidation: performance, practice, and pitfalls. In AFCEE Technology Transfer Workshop, San Antonio, Texas.

Calamari, D., Galassi, S., Setti, F., Vighi, M. (1983). Toxicity of selected chlorobenzenes to aquatic organisms. Chemosphere, 12(2), 253-262.

Cuozzo, S.A., Sineli, P.E., Costa, J.D., Tortella, G., (2018). Streptomyces sp is a powerful biotechnological tool for the biodegradation of HCH isomers: biochemical and molecular basis. Critical Reviews in Biotechnology 38, 719-728.

Deng, J., Shao, Y., Gao, N., Deng, Y., Zhou, S., Hu, X. (2013). Thermally activated persulfate (TAP) oxidation of antiepileptic drug carbamazepine in water. Chemical Engineering Journal, 228, 765-771.

Devi, P., Das, U., Dalai, A. K. (2016). In-situ chemical oxidation: principle and applications of peroxide and persulfate treatments in wastewater systems. Science of the Total Environment, 571, 643-657.

Dominguez, C. M., Oturan, N., Romero, A., Santos, A., Oturan, M. A. (2018a). Removal of organochlorine pesticides from lindane production wastes by electrochemical oxidation. Environmental Science and Pollution Research, 25(35), 34985-34994.

Dominguez, C. M., Oturan, N., Romero, A., Santos, A., Oturan, M. A. (2018b). Removal of lindane wastes by advanced electrochemical oxidation. Chemosphere, 202, 400-409.

Dominguez, C. M., Romero, A., Fernandez, J., Santos, A. (2018c). In situ chemical reduction of chlorinated organic compounds from lindane production wastes by zero valent iron microparticles. Journal of water process engineering, 26, 146-155.

Dominguez, C. M., Romero, A., Santos, A. (2019). Selective removal of chlorinated organic compounds from lindane wastes by combination of nonionic surfactant soil flushing and Fenton oxidation. Chemical Engineering Journal, 376, 120009.

Fernández, J., Arjol, M. A., Cacho, C. (2013). POP-contaminated sites from HCH production in Sabiñánigo, Spain. Environmental Science and Pollution Research, 20(4), 1937-1950.

Furman, O. S., Teel, A. L., Ahmad, M., Merker, M. C., Watts, R. J. (2011). Effect of basicity on persulfate reactivity. Journal of Environmental Engineering, 137(4), 241-247.

Ghauch, A., Tuqan, A. M., Kibbi, N. (2012). Ibuprofen removal by heated persulfate in aqueous solution: a kinetics study. Chemical engineering journal, 197, 483-492.

Goulden, P. D., Anthony, D. H. J. (1978). Kinetics of uncatalyzed peroxydisulfate oxidation of organic material in fresh water. Analytical Chemistry, 50(7), 953-958.

Huang, K. C., Couttenye, R. A., Hoag, G. E. (2002). Kinetics of heat-assisted persulfate oxidation of methyl tert-butyl ether (MTBE). Chemosphere, 49(4), 413-420.

Huang, K. C., Zhao, Z., Hoag, G. E., Dahmani, A., Block, P. A. (2005). Degradation of volatile organic compounds with thermally activated persulfate oxidation. Chemosphere, 61(4), 551-560.

Ike, I. A., Linden, K. G., Orbell, J. D., Duke, M. (2018). Critical review of the science and sustainability of persulphate advanced oxidation processes. Chemical Engineering Journal, 338, 651-669.

Ji, Y., Dong, C., Kong, D., Lu, J., Zhou, Q. (2015). Heat-activated persulfate oxidation of atrazine: implications for remediation of groundwater contaminated by herbicides. Chemical Engineering Journal, 263, 45-54.

Joo, S. H., Zhao, D. (2008). Destruction of lindane and atrazine using stabilized iron nanoparticles under aerobic and anaerobic conditions: effects of catalyst and stabilizer. Chemosphere, 70(3), 418-425.

Kaiser, K. L., Palabrica, V. S. (1991). Photobacterium phosphoreum toxicity data index. Water Quality Research Journal, 26(3), 361-431.

Karlaganis, G., Marioni, R., Sieber, I., Weber, A., (2001). The elaboration of the 'Stockholm Convention' on persistent organic pollutants (POPs): A negotiation process fraught with obstacles and opportunities. Environmental Science and Pollution Research 8, 216-221.

Khan, S., Han, C., Khan, H. M., Boccelli, D. L., Nadagouda, M. N., Dionysiou, D. D. (2017). Efficient degradation of lindane by visible and simulated solar light-assisted S-TiO2/peroxymonosulfate process: kinetics and mechanistic investigations. Molecular Catalysis, 428, 9-16.

Kolthoff, I. M., Miller, I. K. (1951). The chemistry of persulfate. I. The kinetics and mechanism of the decomposition of the persulfate ion in aqueous medium1. Journal of the American Chemical Society, 73(7), 3055-3059.

Krembs, F. J., Siegrist, R. L., Crimi, M. L., Furrer, R. F., Petri, B. G. (2010). ISCO for groundwater remediation: analysis of field applications and performance. Groundwater Monitoring & Remediation, 30(4), 42-53.

Lallas, P.L. (2001). The Stockholm Convention on persistent organic pollutants. American Journal of International Law 95, 692-708

Liang C, Lei J. (2015). Identification of active radical species in alkaline persulfate oxidation. Water Environ Res; 87:656-9.

Liang, C. J., Bruell, C. J., Marley, M. C., Sperry, K. L. (2003). Thermally activated persulfate oxidation of trichloroethylene (TCE) and 1, 1, 1-trichloroethane (TCA) in aqueous systems and soil slurries. Soil and sediment contamination: An international journal, 12(2), 207-228.

Liang, C., Bruell, C. J. (2008). Thermally activated persulfate oxidation of trichloroethylene: experimental investigation of reaction orders. Industrial & Engineering Chemistry Research, 47(9), 2912-2918.

Liang, C., Su, H. W. (2009). Identification of sulfate and hydroxyl radicals in thermally activated persulfate. Industrial & Engineering Chemistry Research, 48(11), 5558-5562.

Lominchar, M. A., Lorenzo, D., Romero, A., Santos, A. (2018). Remediation of soil contaminated by PAHs and TPH using alkaline activated persulfate enhanced by surfactant addition at flow conditions. Journal of Chemical Technology & Biotechnology, 93(5), 1270-1278.

Lorenzo D, García-Cervilla R, Romero A, Santos A. (2020). Partitioning of chlorinated organic compounds from dense non-aqueous phase liquids and contaminated soils from lindane production wastes to the aqueous phase. Chemosphere; 239.

Luo, Q.S. (2014). Oxidative treatment of aqueous monochlorobenzene with thermally-activated persulfate. Frontiers of Environmental Science & Engineering. 8(2): p. 188-194.

Ma, J., Li, H., Chi, L., Chen, H., Chen, C. (2017). Changes in activation energy and kinetics of heat-activated persulfate oxidation of phenol in response to changes in pH and temperature. *Chemosphere*, *189*, 86-93.

Ma, J., Yang, Y., Jiang, X., Xie, Z., Li, X., Chen, C., Chen, H. (2018). Impacts of inorganic anions and natural organic matter on thermally activated persulfate oxidation of BTEX in water. Chemosphere, 190, 296-306.

Madaj, R., Sobiecka, E., Kalinowska, H., (2018). Lindane, kepone and pentachlorobenzene: chloropesticides banned by Stockholm convention. International Journal of Environmental Science and Technology 15, 471-480.

Matzek, L. W. and Carter, K. E. (2016). Activated persulfate for organic chemical degradation: a review. Chemosphere, 151, 178-188.

Navarro, J. S., López, C., García, A. P. (2000). Characterization of groundwater flow in the Bailin hazardous waste-disposal site (Huesca, Spain). Environmental Geology, 40(1-2), 216-222.

Nolan, K., Kamrath, J., Levitt, J. (2012). Lindane toxicity: a comprehensive review of the medical literature. Pediatric Dermatology, 29(2), 141-146.

Rodriguez, S., Santos, A., Romero, A., Vicente, F. (2012). Kinetic of oxidation and mineralization of priority and emerging pollutants by activated persulfate. Chemical engineering journal, 213, 225-234.

Romero, A., Santos, A., Vicente, F., González, C. (2010). Diuron abatement using activated persulphate: effect of pH, Fe (II) and oxidant dosage. Chemical Engineering Journal, 162(1), 257-265.

Santos, A., Fernandez, J., Guadaño, J., Lorenzo, D., Romero, A. (2018a). Chlorinated organic compounds in liquid wastes (DNAPL) from lindane production dumped in landfills in Sabiñanigo (Spain). Environmental pollution, 242, 1616-1624.

Santos, A., Fernandez, J., Rodriguez, S., Dominguez, C. M., Lominchar, M. A., Lorenzo, D., Romero, A. (2018b). Abatement of chlorinated compounds in groundwater contaminated by HCH wastes using ISCO with alkali activated persulfate. Science of the Total Environment, 615, 1070-1077.

Santos, A., Lorenzo, D., Dominguez, C. M. (2019). Persulfate in the remediation of soil and groundwater contaminated by organic compounds. Springer. Electrochemically

Assisted Remediation of Contaminated Soils: Fundamentals, Technologies, Combined Processes and Pre-Pilot and Scale-Up Applications. Springer Science +Business Media. In press

Santos, A., Yustos, P., Quintanilla, A., Garcia-Ochoa, F., Casas, J. A., Rodriguez, J. J. (2004). Evolution of toxicity upon wet catalytic oxidation of phenol. Environmental science & technology, 38(1), 133-138.

Siegrist, R. L., Crimi, M., Simpkin, T.J. (2011). In Situ Chemical Oxidation for Groundwater Remediation, ed. R.U. C. Herb Ward., New York: Springer-Verlag New York.

Sra, K. S., Thomson, N. R., Barker, J. F. (2014). Stability of activated persulfate in the presence of aquifer solids. Soil and Sediment Contamination: An International Journal, 23(8), 820-837.

Tsitonaki, A., Petri, B., Crimi, M., Mosbæk, H., Siegrist, R. L., Bjerg, P. L. (2010). In situ chemical oxidation of contaminated soil and groundwater using persulfate: a review. Critical Reviews in Environmental Science and Technology, 40(1), 55-91.

Usman, M., Tascone, O., Faure, P., Hanna, K. (2014). Chemical oxidation of hexachlorocyclohexanes (HCHs) in contaminated soils. Science of the Total Environment, 476, 434-439.

Vega M, D R, Uotil E. (2017). Lindane (persistant organic pollutant) in the EU. ERA Consult Madrid ERA - Directorate-General for Internal Policies of the Union.

Vijgen, J., Abhilash, P. C., Li, Y. F., Lal, R., Forter, M., Torres, J., Weber, R. (2011). Hexachlorocyclohexane (HCH) as new Stockholm Convention POPs—a global

perspective on the management of Lindane and its waste isomers. Environmental Science and Pollution Research, 18(2), 152-162.

Vijgen, J., Abhilash, P., Li, Y.F., Lal, R., Forter, M., Torres, J., Singh, N., Yunus, M., Tian, C., Schäffer, A., (2011). Hexachlorocyclohexane (HCH) as new Stockholm Convention POPs—a global perspective on the management of Lindane and its waste isomers. Environmental Science and Pollution Research 18, 152-162.

Wacławek, S., Lutze, H. V., Grübel, K., Padil, V. V., Černík, M., Dionysiou, D. D. (2017). Chemistry of persulfates in water and wastewater treatment: a review. Chemical Engineering Journal, 330, 44-62.

Waldemer, R. H., Tratnyek, P. G., Johnson, R. L., Nurmi, J. T. (2007). Oxidation of chlorinated ethenes by heat-activated persulfate: kinetics and products. Environmental Wang, L., Peng, L., Xie, L., Deng, P., Deng, D. (2017). Compatibility of surfactants and thermally activated persulfate for enhanced subsurface remediation. Environmental science & technology, 51(12), 7055-7064.

Wang, J., Wang, S. (2018). Activation of persulfate (PS) and peroxymonosulfate (PMS) and application for the degradation of emerging contaminants. Chemical Engineering Journal, 334, 1502-1517.

Yen, C. H., Chen, K. F., Kao, C. M., Liang, S. H., Chen, T. Y. (2011). Application of persulfate to remediate petroleum hydrocarbon-contaminated soil: Feasibility and comparison with common oxidants. Journal of hazardous materials, 186(2-3), 2097-2102.

Zhao, L., Hou, H., Fujii, A., Hosomi, M., Li, F. (2014). Degradation of 1, 4-dioxane in water with heat-and Fe 2+-activated persulfate oxidation. Environmental Science and Pollution Research, 21(12), 7457-7465.

Zhou, R., Li, T., Su, Y., Li, C., Jin, X., Ren, H. (2019). Removal of sulfanilic acid from wastewater by thermally activated persulfate process: oxidation performance and kinetic modeling. Journal of Chemical Technology & Biotechnology, 94(10), 3208-3216.

Zhu, C., Zhu, F., Dionysiou, D. D., Zhou, D., Fang, G., Gao, J. (2018). Contribution of alcohol radicals to contaminant degradation in quenching studies of persulfate activation process. Water research, 139, 66-73.

Supplementary Material

SM Table 1. Operating conditions of the experimental runs

		$C_{COCs,0}$ (mg L^{-1})	T (ºC)	$C_{PS,0}$ (g L^{-1})	C_{PS}/C_{PS}^{stq}	pH_0
PS stability	R1	0	30	40	-	3
	R2	0	40	40	-	3
	R3	0	50	40	-	3
COCs volatility	R4	57.53	30	0	-	6.5
	R5	57.53	40	0	-	6.5
	R6	57.53	50	0	-	6.5
COCs degradation by TAP: effect of Temperature	R7	57.53	**30**	40	34	3
	R8	57.53	**40**	40	34	3
	R9	57.53	**50**	40	34	3
COCs degradation by TAP: effect of PS concentration	R10	57.53	40	**2**	2.1	3.6
	R11	57.53	40	**5**	4.2	3.4
	R12	57.53	40	**10**	8.5	3.3
	R13	57.53	40	**20**	17	3.2
	R9	57.53	50	**40**	34	3

SM Table 2. Stoichiometric oxidation reactions between PS and the different families of COCs (r_1-r_9)

$r_1: C_6H_5Cl\ (CB) + 12\ H_2O + 29\ SO_4^{\cdot-} \rightarrow 6\ CO_2 + Cl^- + 30\ H^+ + 29\ (SO_4)^{2-}$
$r_2: C_6H_4Cl_2\ (DCB) + 12\ H_2O + 26\ SO_4^{\cdot-} \rightarrow 6\ CO_2 + 2\ Cl^- + 28\ H^+ + 26\ (SO_4)^{2-}$
$r_3: C_6H_3Cl_3\ (TCB) + 12\ H_2O + 24\ SO_4^{\cdot-} \rightarrow 6\ CO_2 + 3\ Cl^- + 27\ H^+ + 24\ (SO_4)^{2-}$
$r_4: C_6H_2Cl_4(TetraCB) + 12\ H_2O + 22\ SO_4^{\cdot-} \rightarrow 6\ CO_2 + 4\ Cl^- + 26\ H^+ + 22\ (SO_4)^{2-}$
$r_5: C_6H_5Cl_5(PentaCX) + 12\ H_2O + 24\ SO_4^{\cdot-} \rightarrow 6\ CO_2 + 5\ Cl^- + 29\ H^+ + 24\ (SO_4)^{2-}$
$r_6: C_6H_4Cl_6\ (HexaCX) + 12\ H_2O + 22\ SO_4^{\cdot-} \rightarrow 6\ CO_2 + 6\ Cl^- + 28\ H^+ + 22\ (SO_4)^{2-}$
$r_7: C_6H_5Cl_7(HeptaCX) + 12\ H_2O + 22\ SO_4^{\cdot-} \rightarrow 6\ CO_2 + 7\ Cl^- + 29\ H^+ + 22\ (SO_4)^{2-}$
$r_8: C_6HCl_5\ (PCB) + 12\ H_2O + 20\ SO_4^{\cdot-} \rightarrow 6\ CO_2 + 5\ Cl^- + 25\ H^+ + 20\ (SO_4)^{2-}$
$r_9: C_6H_6Cl_6\ (HCH) + 12\ H_2O + 24\ SO_4^{\cdot-} \rightarrow 6\ CO_2 + 6\ Cl^- + 30\ H^+ + 24\ (SO_4)^{2-}$

SM Table 3. Information about the COCs identified in the starting polluted water: name of the COC, chemical formula, the acronym used and concentration values.

COC	Chemical formula	Acronym	C_j $(mg\ L^{-1})$
chlorobenzene	C_6H_5Cl	CB	25.76
1,3-dichlorobenzene	$C_6H_4Cl_2$	1,3 DCB	b.d.l.
1,4-dichlorobenzene	$C_6H_4Cl_2$	1,4 DCB	3.21
1,2-dichlorobenzene	$C_6H_4Cl_2$	1,2 DCB	2.33
1,3,5-trichlorobenzene	$C_6H_3Cl_3$	1,3,5 TCB	b.d.l
1,2,4-trichlorobenzene	$C_6H_3Cl_3$	1,2,4 TCB	2.39
1,2,3-trichlorobenzene	$C_6H_3Cl_3$	1,2,3 TCB	0.19
1,2,4,5 - 1,2,3,5-tetrachlorobenzene	$C_6H_2Cl_4$	TetraCB (1,2,4,5 + 1,2,3,5)	0.23
1,2,3,4 tetrachlorobenzene	$C_6H_2Cl_4$	TetraCB (1,2,3,4)	0.37
γ-pentachlorocyclohexene	$C_6H_5Cl_5$	γ–PentaCX	2.40
1,2,3,4,5 pentachlorobenzene	C_6HCl_5	PentaCB	0.02
δ-Pentachlorocyclohexene	$C_6H_5Cl_5$	δ-PentaCX	2.49
θ-Pentachlorocyclohexene	$C_6H_5Cl_5$	θ-PentaCX	b.d.l
Hexachlorocyclohexene	$C_6H_4Cl_6$	HexaCX-a	0.56
β-Pentachlorocyclohexene	$C_6H_5Cl_5$	β-PentaCX	b.d.l
η-Pentachlorocyclohexene	$C_6H_5Cl_5$	η-Penta CX	1.29
Hexachlorocyclohexene	$C_6H_4Cl_6$	HexaCX-b	b.d.l
Hexachlorocyclohexene	$C_6H_4Cl_6$	HexaCX-c	b.d.l
α-hexachlorocyclohexane	$C_6H_6Cl_6$	α-HCH	1.10
Hexachlorocyclohexene	$C_6H_4Cl_6$	HexaCX-d	b.d.l
β-hexachlorocyclohexane	$C_6H_6Cl_6$	β-HCH	b.d.l
γ-hexachlorocyclohexane	$C_6H_6Cl_6$	γ-HCH	4.38
Heptachlorocyclohexane	$C_6H_5Cl_7$	HeptaCH-1	1.59
δ-hexachlorocyclohexane	$C_6H_6Cl_6$	δ-HCH	7.48
ε-hexachlorocyclohexane	$C_6H_6Cl_6$	ε-HCH	0.84
Heptachlorocyclohexane	$C_6H_5Cl_7$	HeptaCH-2	0.53
Heptachlorocyclohexane	$C_6H_5Cl_7$	HeptaCH-3	0.38
		$\sum COCs$	57.53

b.d.l. = below the detection limit

SM Table 4. EC50 values found in the bibliography for the compounds of interest obtained at 15 min of exposure time

Compound	EC50 (mg L^{-1})	Reference
CB	11.52	Kaiser and Palabrica, 1991
1,3 DCB	3.96	Kaiser and Palabrica, 1991
1,2 DCB	4.98	Kaiser and Palabrica, 1991
1,3,5 TCB	14.09	Kaiser and Palabrica, 1991
1,2,3 TCB	2.62	Kaiser and Palabrica, 1991
1,2,4,5 TCB	6.52	Kaiser and Palabrica, 1991
1,2,3,4 TCB	3.34	Kaiser and Palabrica, 1991
1,2,3,5 TCB	3.50	Kaiser and Palabrica, 1991
γ-HCH	5.67	Kaiser and Palabrica, 1991
Formic acid	162	Santos et al., 2004

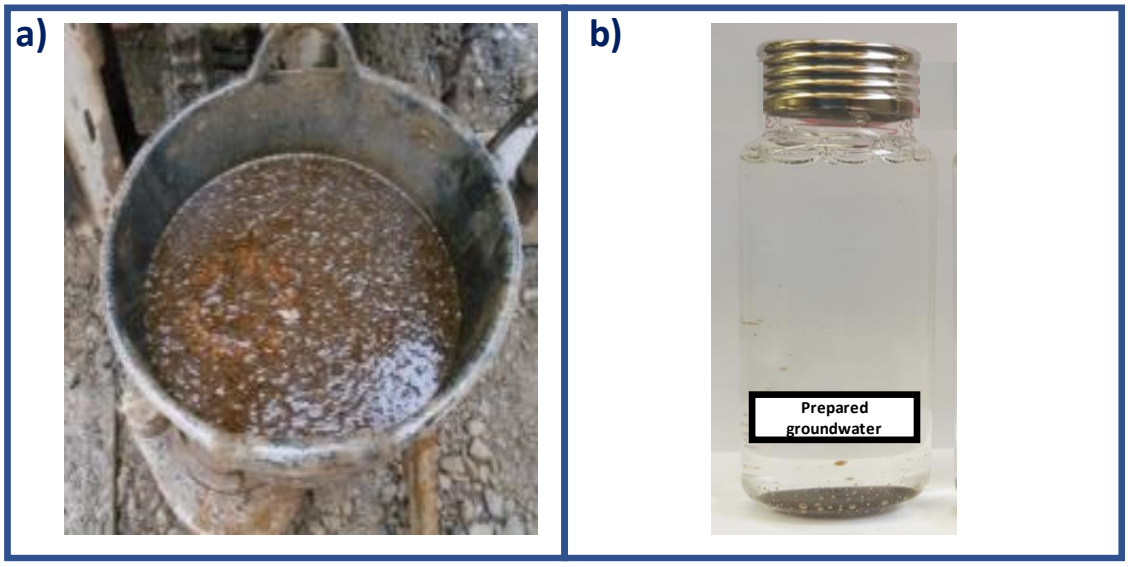

SM Figure 1. Photographs of DNAPL pumped from an extraction well of Sabiñanigo's landfill and the COCs polluted water prepared with this DNAPL.

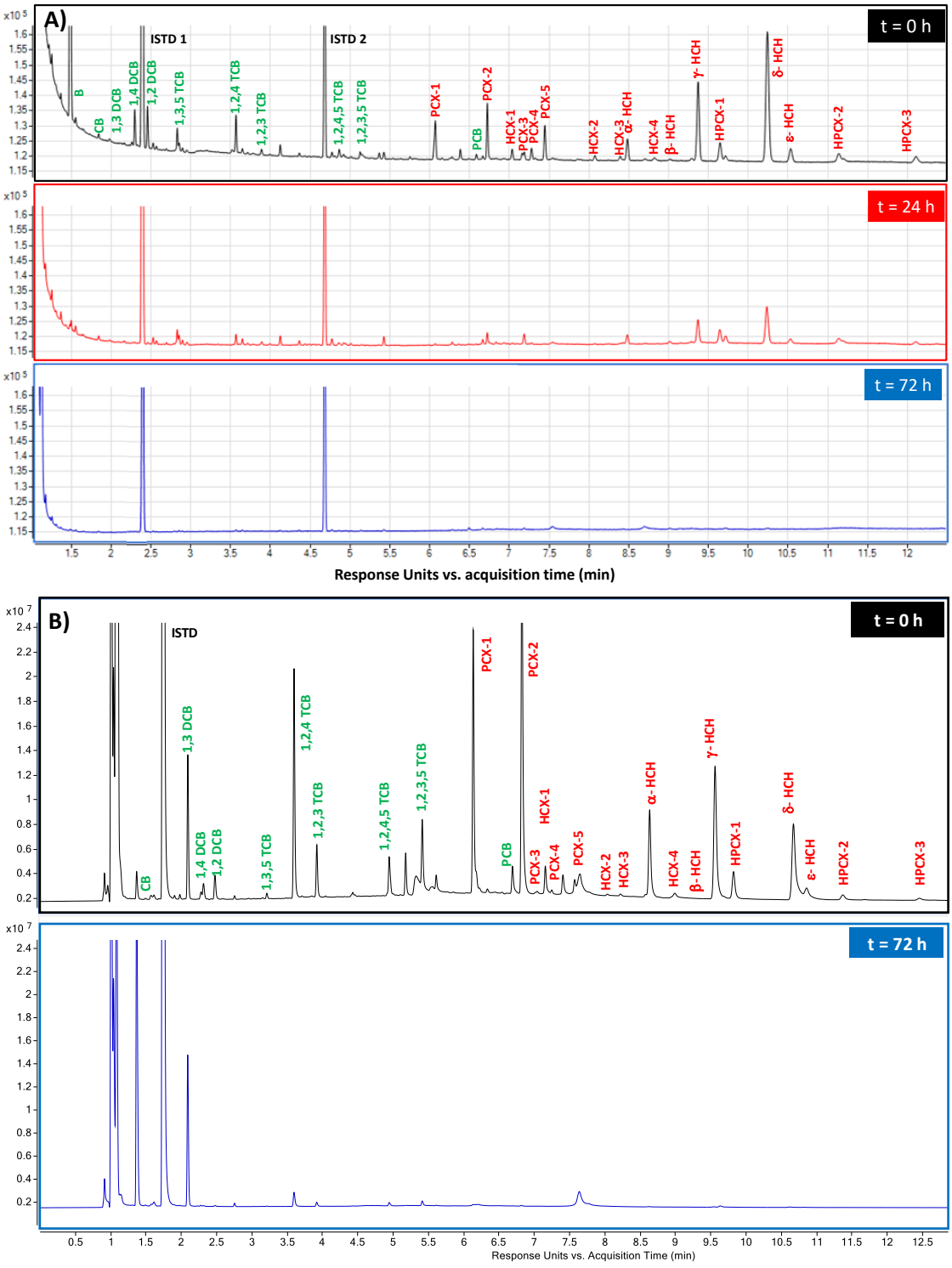

SM Figure 2. GC-FID (A) and GC-ECD (B) chromatograms of the starting polluted water (t=0 h) and treated by thermally activated PS (chlorobenzenes in green, pentachlorocyclohexenes, hexachlorocyclohexenes, HCHs and heptaclorocyclohexanes, in red, and ISTDs, in black) ($COCs_0$=57.53 mg L^{-1}, PS_0=40 g L^{-1}, T =40 ºC).

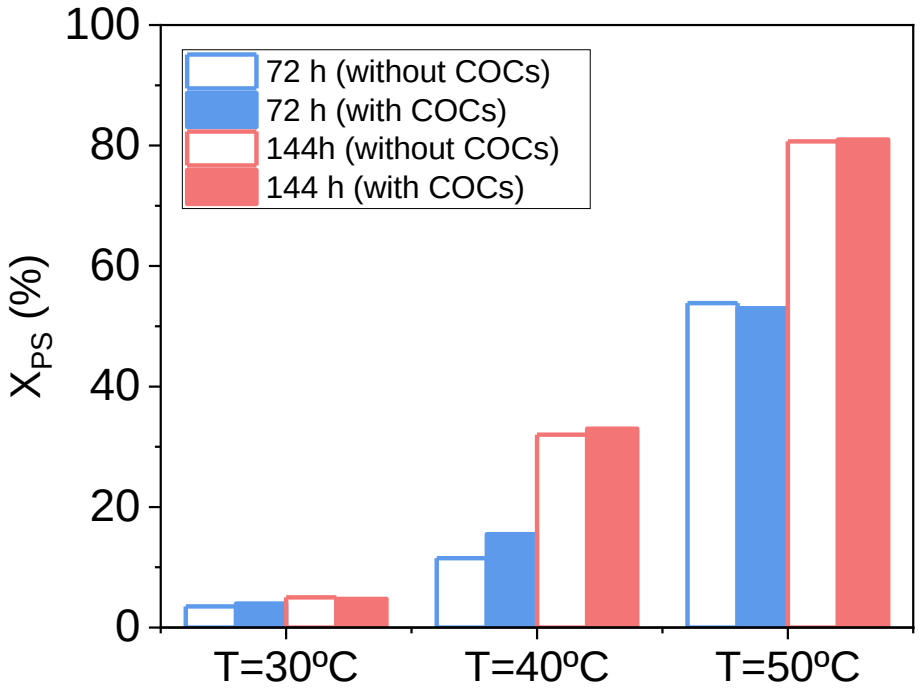

SM Figure 3. PS decomposition in the absence (R1, R2, R3) and presence (R7, R8, R9) of COCs at different temperatures (C_{PS0}=40 g L^{-1}, $COCs_0$=57.53 mg L^{-1} (when applicable)).

Highlights

- COCs (57.53 mg L^{-1}) are efficiently oxidized by thermally activated PS (C_{PS}=10 g L^{-1}, T=40 ºC, 168 h)
- The higher the chlorine content of the COC, the higher resistance towards oxidation
- Increasing the temperature and PS concentration increases the pollutant oxidation rates
- Important unproductive PS consumption by thermal effect
- The kinetic model considers PS concentration, T^a and unproductive PS consumption